Zeta-Based AC-Link Universal Converter

Mojtaba Salehi

Department of Electrical and Computer

Engineering

Northeastern University

Boston, MA, USA

Salehi.mo@northeastern.edu

Masih Khodabandeh
Department of Electrical and Computer
Engineering
Northeastern University
Boston, MA, USA
khodabandeh.m@northeastern.edu

Mahshid Amirabadi
Department of Electrical and Computer
Engineering
Northeastern University
Boston, MA, USA
m.amirabadi@northeastern.edu

Abstract—AC-link universal converters are relatively new topologies that can be used for power conversion from any type of source including, DC or AC, to any type of load. These converters enhance reliability by employing small film capacitors instead of bulky unreliable electrolytic ones. Furthermore, such converters have a high power density due to the possibility of using compact high-frequency transformers when isolation is needed. Universal converters extend the principles of the operation of DC-DC Buck-Boost and Ćuk converters to DC-AC, AC-DC, and AC-AC power conversion systems. In this paper, a new Zeta-based universal converter is proposed, which is capable of stepping up and stepping down the voltage in a wide range. This converter uses an inductor and a capacitor for transferring power from the source to the load. The voltage rating of the capacitor and the current peak of the inductor used in the proposed converter are lower than those of Ćuk-based and Buck-Boost-based universal converters, respectively. Moreover, the proposed topology is a single-stage power converter, which has a higher efficiency compared to conventional two-stage power converters. The principles of the operation of the proposed converter are presented in this paper, and its performance is verified through simulations and experiments.

Keywords—universal converter, ac-ac converter, inverter, rectifier, Ćuk converter, Buck-Boost converter, Zeta converter, high-frequency ac link.

I. INTRODUCTION

Power converters are an integral part of many systems, including renewable energy systems, electric vehicles, and industrial drives. However, conventional DC-link power converters may not be practical for reliability-demanding applications due to frequent failures and the short lifespan of electrolytic capacitors.

Nowadays, due to the increasing electric energy consumption and the advent of different electrical load types, demand for universal converters that can transfer electric power from different types of sources to different kinds of loads is emerging. In recent years AC-link universal converters that are derived from DC-DC converters have received increasing attention due to their unique characteristics. Buck-Boost-based and Ćuk-based universal converters are the most well-known types of these AC link converters [1]-[11].

Single-stage Buck-Boost-based universal converters use an inductor at the link to transfer power. To minimize the size of the inductor, a high current ripple for the inductor can be allowed [1]. The main problem with these topologies is the high link peak current, which increases the conduction losses of the switches. However, these types of converters can use a small capacitor in parallel with the link inductor to realize soft-switching and improve efficiency [2]. In [3], a softswitching Buck-Boost-based universal converter with reduced link peak current is presented to enhance the efficiency of the system. However, this converter experiences a long resonating interval during which no power is transferred, and this can negatively affect the performance of the system. To reduce the duration of the resonating modes, four-quadrant switches can be used instead of two-quadrant switches [4]. However, this will double the number of switches. Universal Buck-Boost-based converters proposed in [1]-[4], use only one inductor for transferring power. In [5], a bidirectional PWM Buck-Boost-based AC-AC converter is proposed, which requires three bulky inductors for the energy transferring process. In [6, 7] a Buck-Boost inverter is proposed to increase the voltage gain in the Buck-Boostbased family of AC-link converters. However, they suffer from high current spikes and low efficiency. In [8], another single-stage three-phase Buck-Boost-derived inverter is introduced to increase the voltage gain. The main shortcoming of this inverter is that it needs a large inductor and suffers from low efficiency.

In Buck-Boost-based AC-link converters, achieving high efficiency is typically challenging. In all the abovementioned configurations, an inductor is the main energy transferring element, which lowers the overall power density of the system. Another family of universal converters is the Ćuk-based universal converters in which a small series film capacitor is employed as the energy transferring element. A Cuk-derived three-phase AC-AC converter that uses a small series film capacitor instead of an electrolytic one is presented in [9]. In [10], by adding a small inductor in series with the link capacitor, a soft-switching Cuk-based PVinverter is developed. The link capacitor has a high peak voltage in Ćuk-based universal converters. To solve this problem a single-stage Zeta-based inverter and a SEPICbased rectifier, in which the capacitor has a lower peak voltage are proposed in [11].

This paper proposes a novel Zeta-based universal converter that can be configured as a rectifier, an AC-AC converter, or an inverter. The proposed topology not only eliminates the bulky electrolytic capacitors but also increases power density by using lightweight high-frequency transformers instead of heavy line-frequency transformers. Compared to Ćuk-based and Buck-Boost-based universal converters, the Zeta-based universal converter has lower capacitor peak voltage and lower inductor peak current, respectively.

This article is organized as follows: The topologies and operating principles are introduced in section II. After that, the design and analysis are discussed in section III. The simulation and experimental results are presented in section IV. Finally, the paper is summarized in section V.

II. OPERATING PRINCIPLES

The operation principles of the three-phase Zeta rectifier and the Zeta-based three-phase AC-AC converter are presented in parts (A) and (B) of this section, respectively.

A. Three-phase Zeta Rectifier

The proposed three-phase Zeta rectifier is shown in Fig. 1(a). The transformer is optional, and in the isolated converter, the isolation is provided with a high-frequency transformer (HFT). In this converter, the link capacitor is a small film capacitor, unlike conventional DC-link converters that use unreliable electrolytic capacitors. To clarify the system behavior during different conditions, the link voltage, link current, and input inductor voltage waveforms are depicted in Fig. 1(b).

In each cycle, two main operating modes exist. The first mode is transferring power from the input inductor (L_{in}) to the link capacitor. Mode 2 is a de-energizing mode from the link capacitor to the DC load. During the second mode, where the link capacitor is discharging to the output load, the input side inductor (L_{in}) charges from the input AC source within two different sub-modes.

The behavior of the proposed non-isolated rectifier during different modes is shown in Fig. 2. In this figure, it is assumed that I_A^{ref} , the reference current of phase A, is positive and has the maximum absolute value among three-phase currents. I_B^{ref} and I_C^{ref} , are negative and the absolute value of I_C^{ref} is smaller than I_B^{ref} . It is obvious that based on the absolute

values of input currents, we have different zones and switching patterns.

As shown in Fig. 2(a), during the first mode, input switches are off, and the link capacitor will be charged by the input inductor current (I_{in}) through the DC-side diode. The link voltage increases during this mode until the desired amount of power is transferred. It should be noted that during this mode, all unfiltered input currents are equal to zero. Once the link is charged sufficiently, the proper input switches are turned on, and mode 2 starts.

In mode 2 (Fig. 2(b)), the link capacitor is discharged to the DC load with current I_{out} , and the link voltage decreases. Simultaneously in the first sub-mode, Q1 and Q5 are turned on such that the highest line-to-line voltage (V_{AB}) appears across the input inductor (L_{in}). During this mode, voltage $V_{AB} + V_{link}$ appears across the DC-side diode. As soon as the average value of the second-highest current ($I_B^{average}$) meets its reference value (I_B^{ref}), the switching status will change, and I_C will flow to the input inductor (Fig. 2(c)). In this case, switch Q6 is turned on, switch Q1 remains ON, and switch Q5 is turned off. During this sub-mode, the voltage over the input inductor (L_{in}) is equal to V_{AC} . This sub-mode continues until $I_C^{average}$ meets I_C^{ref} . During this last mode, the unfiltered output voltage is equal to $V_{AC} + V_{link}$.

B. Zeta-Based Three-Phase AC-AC Converter

The isolated Zeta-based three-phase AC-AC converter with a small film capacitor and an optional high-frequency transformer is shown in Fig. 3(a). The link voltage, link current, and input inductor voltage waveforms in a typical switching cycle of the proposed topology are shown in Fig. 3(b) to clarify the system behavior. The behavior of the proposed non-isolated AC-AC converter during different modes is shown in Fig. 4.

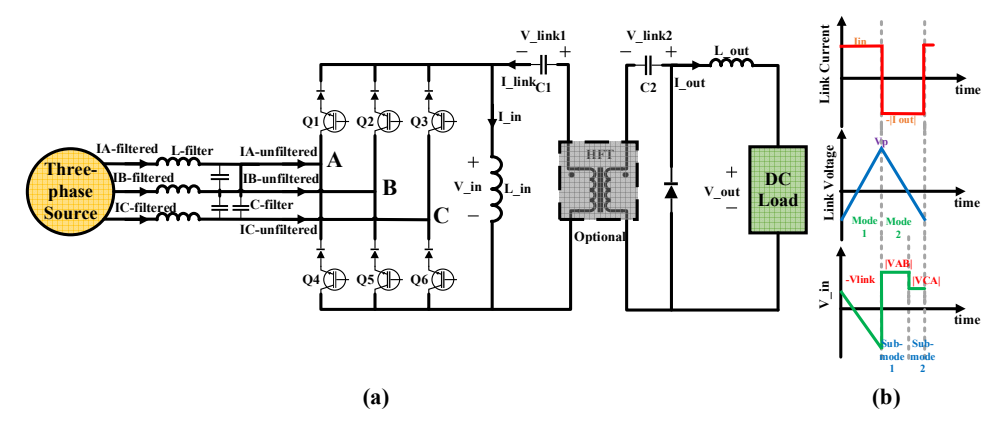


Fig. 1. (a) Isolated Zeta-based three-phase rectifier (b) Link capacitor voltage, link capacitor current, and input inductor voltage waveforms in the Zeta-based rectifier.

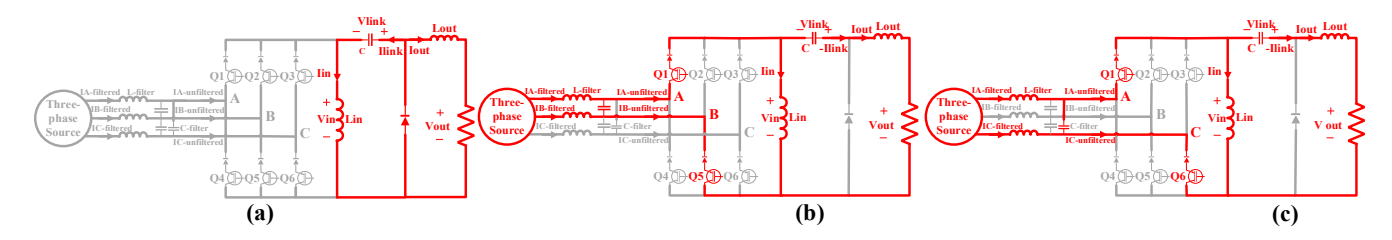


Fig. 2. Behavior of the three-phase Zeta rectifier during: (a) mode 1, (b) mode 2 (sub-mode 1), (c) mode 2 (sub-mode 2).

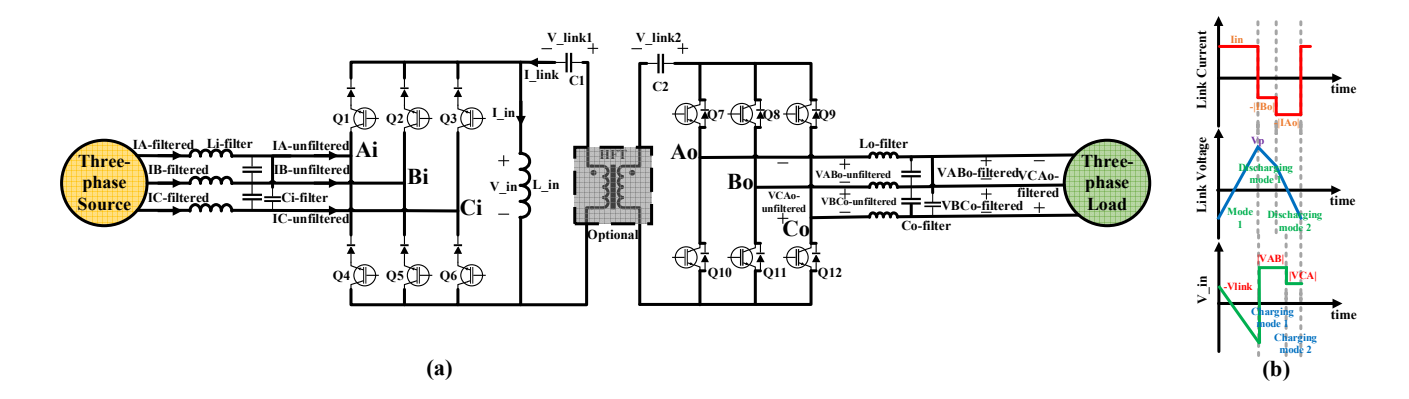


Fig. 3. (a) Zeta-based three-phase AC-AC converter (b) Link current, link voltage, and input inductor voltage waveforms in Zeta-based three-phase AC-AC converter.

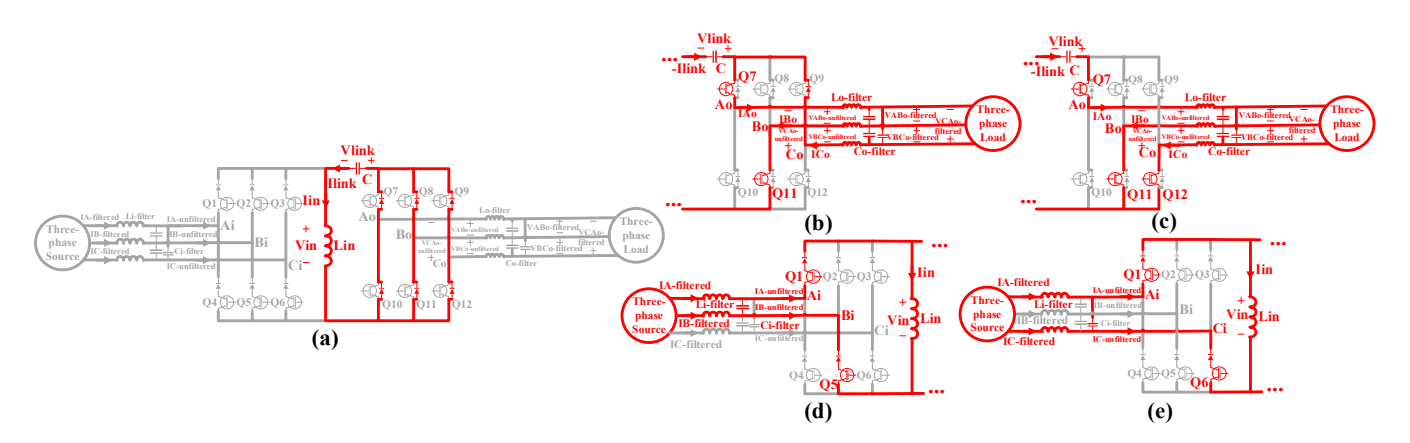


Fig. 4. Behavior of the three-phase AC-AC converter during: (a) mode 1, (b) capacitor discharging mode 1, (c) capacitor discharging mode 2, (d) inductor charging mode 1, and (e) inductor charging mode 2.

Each switching cycle consists of five operating modes. The first mode is transferring power from the input inductor (L_{in}) to the link capacitor. After mode 1, the first link capacitor discharging mode and the first input inductor charging mode start simultaneously. In a three-phase AC-AC configuration, there are two modes for link capacitor discharging and two modes for input inductor charging.

In Figs. 3 and 4, it is assumed that V_{ABO}^{ref} , the reference of the output voltage across phases AB, is positive and has the maximum absolute value among the three-phase output line-to-line voltages. The other line-to-line reference voltages, V_{BCO}^{ref} and V_{CAO}^{ref} , are negative and the absolute value of V_{CAO}^{ref} is

smaller than V_{BCO}^{ref} . The polarities and values of the output line-to-line voltages determine which switches at the output side need to be turned on or off during each cycle. It is also assumed that I_A^{ref} , the reference current of phase A, is positive and has the maximum absolute value among three-phase currents. I_B^{ref} and I_C^{ref} , are negative and the absolute value of I_C^{ref} is smaller than I_B^{ref} . This information is used to determine the input-side switching pattern. It is obvious that based on the absolute values of input currents, we have different zones and switching patterns. Tables I and II show 12 different zones for the input and output sides in the AC-AC converter.

TABLE I. DIFFERENT ZONES FOR THE OUTPUT-SIDE IN AC-AC CONVERTER

Zone	1	2	3	4	5	6	7	8	9	10	11	12
Maximum line-to-line voltage	V_{AB}	V_{AB}	$-V_{CA}$	$-V_{CA}$	V_{BC}	V_{BC}	$-V_{AB}$	$-V_{AB}$	V_{CA}	V_{CA}	$-V_{BC}$	$-V_{BC}$
Second line-to-line voltage	$-V_{BC}$	$-V_{CA}$	V_{AB}	V_{BC}	$-V_{CA}$	$-V_{AB}$	V_{BC}	V_{CA}	$-V_{AB}$	$-V_{BC}$	V_{CA}	V_{AB}
Minimum line-to-line voltage	$-V_{CA}$	$-V_{BC}$	V_{BC}	V_{AB}	$-V_{AB}$	$-V_{CA}$	V_{CA}	V_{BC}	$-V_{BC}$	$-V_{AB}$	V_{AB}	V_{CA}

TABLE II. DIFFERENT ZONES FOR THE INPUT-SIDE IN AC-AC CONVERTER

Zone	1	2	3	4	5	6	7	8	9	10	11	12
Maximum line-to-line voltage	I_A	I_A	$-I_A$	$-I_A$	I_B	I_B	$-I_B$	$-I_B$	I_C	I_C	$-I_C$	$-I_C$
Second line-to-line voltage	$-I_B$	$-I_C$	I_B	I_C	$-I_A$	$-I_C$	I_A	I_C	$-I_A$	$-I_B$	I_A	I_B
Minimum line-to-line voltage	$-I_C$	$-I_B$	I_C	I_B	$-I_C$	$-I_A$	I_C	I_A	$-I_B$	$-I_A$	I_B	I_A

As shown in Fig. 4(a), during the first mode, all switches are off, and the link capacitor will be charged by the input inductor current (I_{in}) through the load-side anti-parallel diodes. The link voltage increases during this mode until the desired amount of power is transferred.

Once the link is charged sufficiently, proper switches from the input and output sides are turned on and the first mode finishes. As depicted in Fig. 4(b), in the first discharging mode, the link capacitor is discharged to the three-phase load with the second-highest load current (I_{Bo}). During this mode, Q7, Q11, and the anti-parallel diode of Q9 conduct the current and discharge the link capacitor. When the average of corresponding output line-to-line voltage (V_{BCO}) meets its reference value ($V_{BCO}^{reference}$), this mode ends and the second capacitor discharging mode initiates.

The second discharging mode discharges the link capacitor with the highest load current ($|I_{Ao}|$ in Fig. 4(c)). During this mode, Q7, Q11, and Q12 are ON to supply the three-phase load. This mode lasts until the remaining energy of the link capacitor discharges to the load. During these two discharging modes, the unfiltered line-to-line voltages and the voltage across the off-state switches at the load side are equal to $V_{in} + V_{link}$, and the value of V_{in} depends on the charging mode status.

Simultaneously in the first charging mode (Fig. 4(d)), Q1 and Q5 conduct such that the highest line-to-line voltage (V_{AB}) appears across the input inductor (L_{in}) . As soon as the average value of the second-highest current $(I_B^{average})$ meets its reference value (I_B^{ref}) , the switching status will change to initiate the second inductor charging mode.

And finally, in the second charging mode (Fig. 4(e)), switches Q1 and Q6 are ON, and the voltage over the input inductor (L_{in}) is equal to V_{CA} . This mode continues until when $I_C^{average}$ meets I_C^{ref} .

It should be noted that the input inductor charging modes and the link capacitor discharging modes are controlled independently and they have different durations, i.e. although the first link capacitor discharging mode and first input inductor charging mode start at the same time they do not end simultaneously; thus, the second link capacitor discharging mode and the second input inductor charging mode do not start simultaneously. In Fig. 3(b) it is assumed that the first input inductor charging mode is longer than the first link capacitor discharging mode.

III. DESIGN AND ANALYSIS

In this section, the design and analysis of the proposed universal converter are presented.

According to (1), the input inductor (L_{in}) can be determined based on the average input inductor voltage after the first mode (V_{in}), the inductor current ripple (ΔI_{in}), link cycle period (T), and the duration of mode 1 (T_1). It should be noted that the average value of I_{in} can be controlled by the duration of T_1 .

$$L_{in} = \frac{V_{in}}{\Delta I_{in}} (T - T_1) \tag{1}$$

For the same frequency and power level, the ripple and peak values of the input inductor current in the proposed topology are lower than the ripple and peak values of the inductor current in Buck-Boost-based universal converters reported in [4].

To determine the maximum voltage across the link capacitor (V_p) , the unfiltered input and output voltages during a cycle are considered. From Fig. 5 one can write:

$$V_{lll} = \frac{1}{2} \left(\frac{\left(V_{in} + V_p \right) \times \left(T - T_1 \right)}{T} \right) \tag{2}$$

$$V_{in} = \frac{1}{2} \left(\frac{(V_{in} + V_p) \times T_1}{T} \right)$$
 (3)

Where V_{lll} is the largest unfiltered line-to-line voltage at the output side. From (2) and (3), the link peak voltage is determined as:

$$V_p = 2V_{lll} + V_{in} \tag{4}$$

It should be noted that the V_{lll} varies between $1.5V_m$ and $\sqrt{3}V_m$, where V_m is the amplitude of the reference line-to-neutral three-phase voltages. In comparison to the equation given in [10], for Ćuk-based converters, the calculated capacitor peak voltage in the proposed converter is smaller.

Using (4) and the link capacitor power formula, which is fully delivered to the load, one can easily design the link capacitor value from (6).

$$P = \frac{1}{2}Cf_{sw}(V_p + V_{in})^2 \tag{5}$$

$$C = \frac{2 \times P_{out}}{f_{sw}(V_p + V_{in})^2} \tag{6}$$

Table III presents a brief comparison between the proposed converter, Buck-Boost-based, and Ćuk-based converters.

For loss and efficiency calculations, it is assumed that the inductors and capacitors are ideal, and the main power loss sources in the proposed converter are the switching power loss (P_{sw}) and conduction losses (P_{cond}) of semiconductor devices.

IV. SIMULATION AND EXPERIMENTAL RESULTS

In this section, the proposed universal converter is evaluated through simulation and experiments. In part (A), simulation results corresponding to a Zeta rectifier is presented. Part (B) presents the simulation results of the three-phase AC-AC Zeta converter. Experimental results corresponding to the Zeta inverter are discussed in part (C). Parameters of the converter are summarized in Table IV. As can be seen, a small film capacitor is employed in the designed converter instead of conventional large electrolytic capacitors.

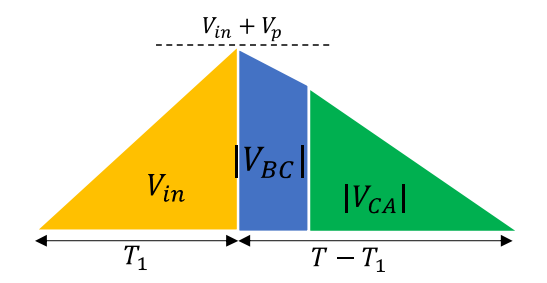


Fig. 5. Unfiltered line-to-line voltages

TABLE III. COMPARSION BETWEEN THE PROPOSED CONVERTER AND THE BUCK-BOOST AND ĆUK CONVERTERS

	Maximum efficiency	Capacitor peak voltage	Inductor peak current
Zeta-based converter	95%	$2V_{lll} + V_{in}$	$2I_{in}$
Buck-boost-based converter [4]	94%	-	$2(I_{in}+I_{out})$
Ćuk-based converter [10]	95%	$2V_{lll} + 2V_{in}$	-

TABLE IV. ZETA-BASED UNIVERSAL CONVERTER PARAMETERS

Link frequency	Power level	Link capacitance	Input inductance	Output DC voltage in the designed Zeta rectifier	Output line-to- line voltage amplitude in the designed AC-AC Zeta converter
55 kHz	1.2 kW	100 nF	500 μΗ	110 V	120 V

A. Zeta Rectifier

Simulation results corresponding to the designed Zeta rectifier are depicted in Figs. 6- 9. Fig. 6 shows the link voltage and link current. As it is evident, the link voltage is negative for a small portion of the cycle to allow using a film capacitor with a lower voltage rating in comparison to Cukbased universal converters. The link peak voltage is about 300 V, which verifies (4) during different modes and zones $(95 V < V_{in} < 200 V$, $100 V < V_{ill} < 120 V$). The input inductor's voltage and current waveforms are depicted in Fig. 7. The current ripple on the input inductor is less than 1A and is smaller than the inductor current ripple in the Buck-Boostbased universal converters. Fig. 8 represents the unfiltered input currents. This figure shows two different charging modes for the input inductor. Fig. 9 demonstrates the DC output voltage and the filtered input currents with the unity power factor and THD of 3% in a 1.2 kW power level.

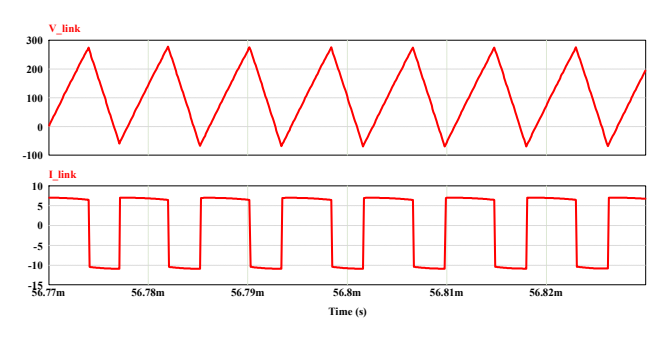


Fig. 6. Link capacitor voltage and current waveforms in the Zeta rectifier (simulation).

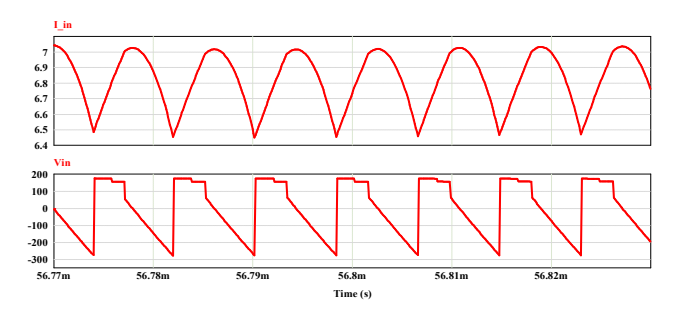


Fig. 7. Input inductor voltage and current waveforms in the Zeta rectifier (simulation).

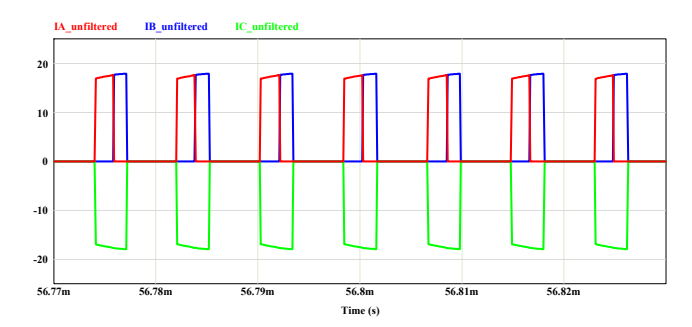


Fig. 8. Unfiltered input currents waveform in the Zeta rectifier (simulation).

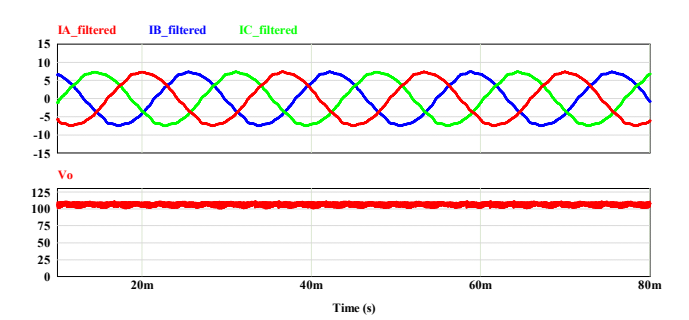


Fig. 9. Filtered input currents and output DC voltage in the Zeta rectifier (simulation).

B. Zeta Three-Phase AC-AC Converter

Simulation results corresponding to the designed threephase AC-AC converter are illustrated in Figs. 10- 12. The link voltage and current are shown in Fig. 10. Similar to the previous case, the link peak voltage is about 300 V, and the minimum value of the link voltage can be negative, which reduces the link peak voltage compared to Cuk-based converters. The unfiltered output voltages and unfiltered input currents are shown in Fig. 11. As mentioned in section II, the input inductor charging modes and the link capacitor discharging modes are controlled independently and they have different durations. For the case shown in Fig. 11, the first input inductor charging mode is longer than the first link capacitor discharging mode. Fig. 12 shows the input inductor voltage and current waveforms with the current ripple of about 0.6A. Fig. 13 shows the output filtered voltages with the unity power factor and THD of 3.5%, and the filtered input currents with THD of 4.8%.

C. Zeta Inverter

A prototype for evaluating the proposed universal converter was fabricated (Fig. 14). Experimental results corresponding to the three-phase inverter operating at 450W power level are illustrated in Figs. 14- 18. Parameters of the system are listed in Table V. Fig. 15 shows the link voltage and current with a 7.5 kHz switching frequency. The input inductor current and voltage are shown in Fig. 16. The unfiltered output voltages are given in Fig. 17. Different discharging modes are clear in this figure. The Filtered output three-phase voltages with a unity power factor are depicted in Fig. 18.

V. CONCLUSION

This paper presented a novel Zeta-based universal converter that can be used as a three-phase rectifier, an inverter, and a three-phase AC-AC converter. In this topology, bulky unreliable electrolytic capacitors used in conventional DC-link converters, are replaced with small

film capacitors. Furthermore, compared to Ćuk-based and Buck-Boost-based universal converters, the link peak voltage and inductor peak current are decreased. Moreover, the capability of using a high-frequency transformer instead of bulky line-frequency transformers can reduce the total size and weight of the system. In this paper, the proposed topology was verified through both simulations and experiments.

TABLE V. ZETA INVERTER PARAMETERS

Power level	Link frequency	Link capacitance	Input Inductance	Output filter inductance
450 w	7.5 kHz	1 μF	500 μΗ	1 mH

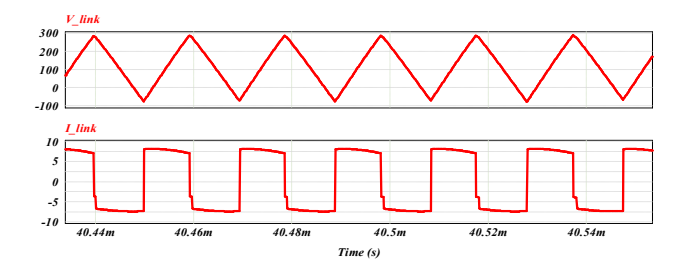


Fig. 10. Link voltage and current in Zeta-based AC-AC converter (simulation).

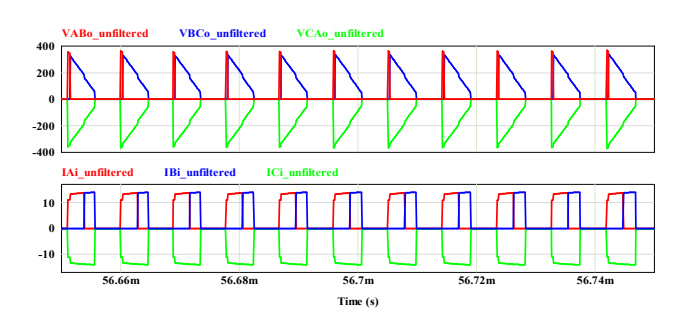


Fig. 11. Unfiltered output voltages and unfiltered input currents in Zeta-based AC-AC converter (simulation).

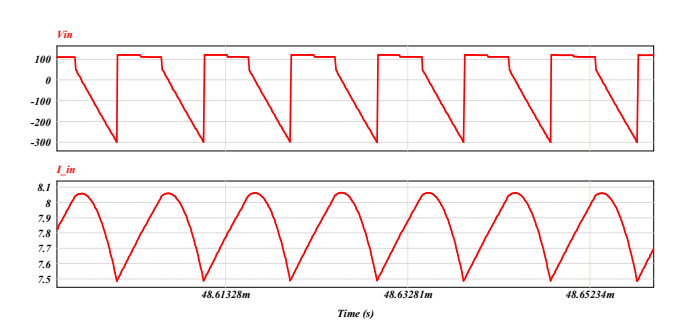


Fig. 12. Input inductor voltage and current waveforms in Zeta-based AC-AC converter (simulation).

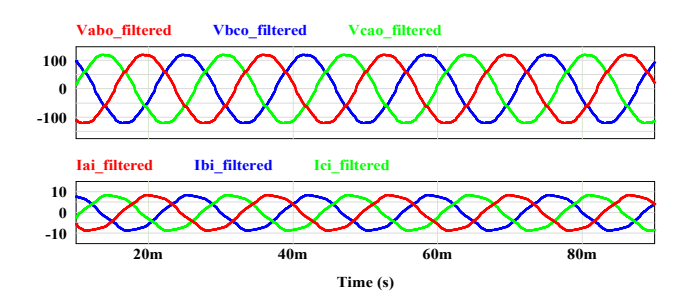


Fig. 13. Three-phase filtered output voltages and three-phase filtered input currents in Zeta-based AC-AC converter (simulation).

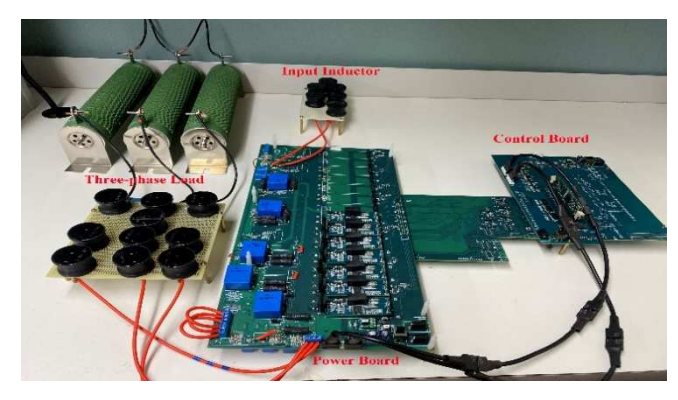


Fig. 14. Experimental setup.

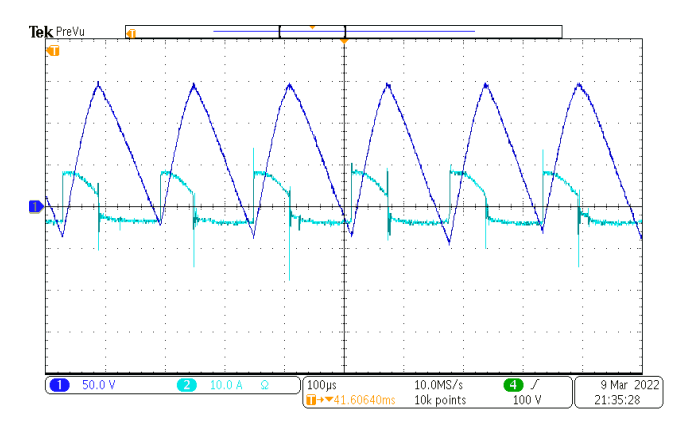


Fig. 15. Link capacitor voltage and current in Zeta inverter (Experimental results).

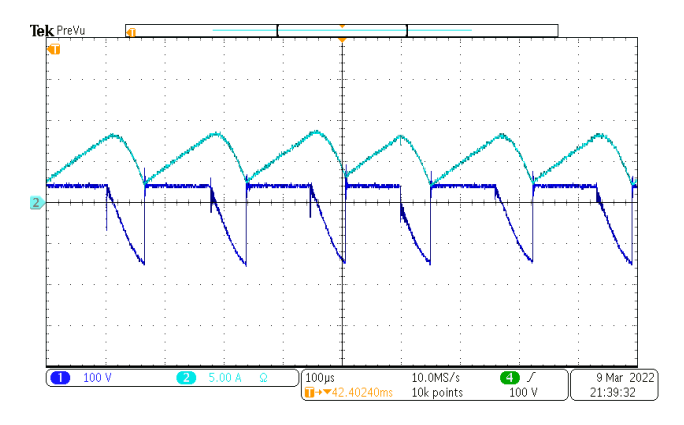


Fig. 16. Input inductor current and voltage in Zeta inverter (Experimental results).

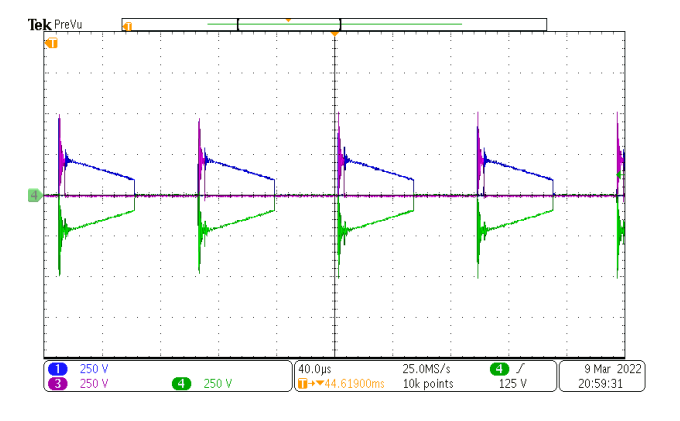


Fig. 17. Unfiltered output voltages in Zeta inverter (Experimental results).

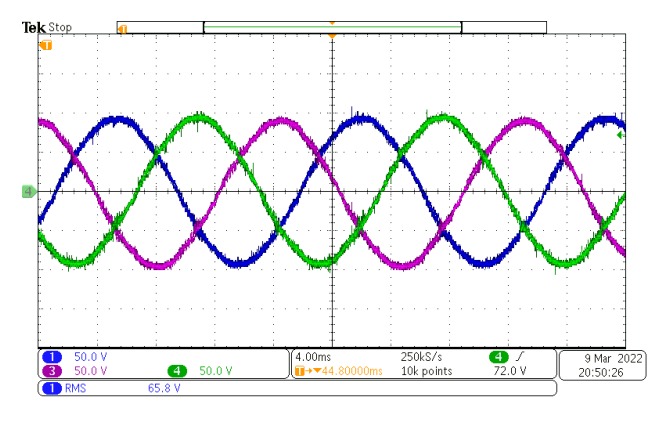


Fig. 18. Filtered output voltages in Zeta inverter (Experimental results).

ACKNOWLEDGMENT

This material is based upon work supported by the National Science Foundation under Grant No. 2047213.

REFERENCES

- L. Kim and G. Cho, "New bilateral zero voltage switching AC/AC converter using high frequency partial-resonant link," in 16th Annual Conference of IEEE Industrial Electronics Society, 1990, pp. 857-862.
- [2] M. Amirabadi, J. Baek, H. A. Toliyat and W. C. Alexander, "Soft-Switching AC-Link Three-Phase AC-AC Buck-Boost Converter," in IEEE Transactions on Industrial Electronics, vol. 62, no. 1, pp. 3-14, Jan. 2015, doi: 10.1109/TIE.2014.2331011.
- [3] K. Mozaffari and M. Amirabadi, "A Highly Reliable and Efficient Class of Single-Stage High-Frequency AC-Link Converters," in IEEE

- Transactions on Power Electronics, vol. 34, no. 9, pp. 8435-8452, Sept. 2019, doi: 10.1109/TPEL.2018.2888583.
- [4] M. Amirabadi, H. A. Toliyat and W. C. Alexander, "A Multiport AC Link PV Inverter With Reduced Size and Weight for Stand-Alone Application," in IEEE Transactions on Industry Applications, vol. 49, no. 5, pp. 2217-2228, Sept.-Oct. 2013, doi: 10.1109/TIA.2013.2262093.
- [5] A. A. Khan, H. Cha, and H. F. Ahmed, "A new reliable three-phase buck-boost AC–AC converter," *IEEE Trans. Ind. Electron.*, vol. 65, no. 2, pp. 1000–1010, Feb. 2018.
- [6] F. Gao, P. C. Loh, R. Teodorescu, F. Blaabjerg, and D. M. Vilathgamuwa, "Topological design and modulation strategy for buck-boost three-level inverters," IEEE Transactions on Power Electronics, vol. 24, no. 7, pp. 1722-1732, 2009.
- [7] F. Gao, P. C. Loh, R. Teodorescu, and F. Blaabjerg, "Diode-Assisted Buck-Boost Voltage-Source Inverters," IEEE Transactions on Power Electronics, vol. 24, no. 9, pp. 2057-2064, 2009.
- [8] A. Darwish, A. M. Massoud, D. Holliday, S. Ahmed, and B. Williams, "Single-stage three-phase differential-mode buck-boost inverters with continuous input current for PV applications," *IEEE Trans. Power Electron.*, vol. 31, no. 12, pp. 8218–8236, Dec. 2016.
- [9] E. Afshari, M. Khodabandeh and M. Amirabadi, "A Single-Stage Capacitive AC-Link AC-AC Power Converter," in IEEE Transactions on Power Electronics, vol. 34, no. 3, pp. 2104-2118, March 2019, doi: 10.1109/TPEL.2018.2841398.
- [10] M. Khodabandeh, E. Afshari, and M. Amirabadi, "A Single-Stage Soft-Switching High-Frequency AC-Link PV Inverter: Design, Analysis, and Evaluation of Si-Based and SiC-Based Prototypes," *IEEE Transactions on Power Electronics*, vol. 34, no. 3, pp. 2312-2326, 2018.
- [11] M. Khodabandeh and M. Amirabadi, "A Soft-switching Single-stage Zeta-/SEPIC-based Inverter/Rectifier," 2020 IEEE Applied Power Electronics Conference and Exposition (APEC).